



Inhibition of prolyl hydroxylase domain (PHD) by JTZ-951 reduces obesity-related diseases in the liver, white adipose tissue, and kidney in mice with a high-fat diet

Hisako Saito¹ · Tetsuhiro Tanaka¹ · Mai Sugahara¹ · Shinji Tanaka¹ · Kenji Fukui^{1,2} · Takeshi Wakashima^{1,2} · Masaomi Nangaku¹

Received: 22 August 2018 / Revised: 16 January 2019 / Accepted: 28 January 2019 / Published online: 5 April 2019

© United States & Canadian Academy of Pathology 2019

Abstract

The epidemic of obesity and its complications is rapidly increasing worldwide. Recent drug discoveries established the utility of prolyl hydroxylase domain (PHD) inhibitors as stabilizers of hypoxia-inducible factors (HIFs) in vivo, which are currently in human clinical studies for the treatment of anemia in chronic kidney disease (CKD). These studies suggest a role for PHD inhibitors in ameliorating obesity and hyperlipidemia. We hypothesized that HIF activation using a PHD inhibitor, JTZ-951, protects from obesity-related diseases in the white adipose tissue (WAT), liver, and kidney in mice fed with high-fat diet (HFD). Eight-week-old, C57BL/6J mice were fed with HFD for 20 weeks with or without JTZ-951 (0.005%; mixed in chow). Body weight and plasma non-high-density lipoprotein (HDL) cholesterol levels were significantly lower in the JTZ-951 group as compared with the vehicle group. PHD inhibition improved liver steatosis, macrophage infiltration into WAT and adipocyte fibrosis. In the kidney, PHD inhibition reduced albuminuria. Histologically, the number of F4/80-positive infiltrating macrophages and mesangial expansion were milder in the JTZ-951 group. Relative mRNA expression of *adiponectin* in WAT was higher in the JTZ-951-treated group and inversely correlated with hepatic steatosis score, adipocyte macrophage aggregation, and albuminuria. Activation of HIF ameliorates multiple obesity-related consequences in mice with HFD. The results of the present study offer the promising view that pharmacological PHD inhibition may be beneficial for the treatment of obesity-related diseases that can be ameliorated by weight loss.

Introduction

Hypoxia-inducible factor (HIF) plays a central role in the hypoxia response. HIF upregulates the transcription of 100–200 target genes related to hypoxic adaptation, such as *erythropoietin (EPO)*, *vascular endothelial growth factor (VEGF)*, and glycolytic enzymes. HIF is a heterodimeric transcription factor consisting of an oxygen-labile α and a

constitutively expressed β subunits. In normoxia, two conserved proline residues in HIF- α are hydroxylated by prolyl hydroxylase domain (PHD). Hydroxylated HIF- α is recognized by the von Hippel–Lindau tumor suppressor protein (pVHL), resulting in immediate proteasomal degradation via polyubiquitination. By contrast, during hypoxia, PHD activity is lost and HIF- α escapes degradation. HIF- α is then able to translocate to the nucleus where it forms a heterodimer with HIF- β . HIF heterodimers bind to hypoxia response elements (HRE) in the regulatory regions of target genes, resulting in transactivation of target genes. HIF- α has 2 major isoforms, HIF-1 α and HIF-2 α . HIF-2 α is a major regulator of erythropoietin expression [1]. Multiple lines of evidence show that HIF activation protects the kidney from injury, particularly acute kidney injury (AKI) [2–4].

HIF coordinates the physiologic response to systemic anemia by altering *EPO* gene expression in the kidney and liver, and by improving uptake and use of iron [5]. Based on these observations, HIF activation is regarded as a promising target for a next-generation erythropoiesis-stimulating agent,

✉ Tetsuhiro Tanaka
tetsu-ty@umin.ac.jp

✉ Masaomi Nangaku
mnangaku-ty@umin.ac.jp

¹ Division of Nephrology and Endocrinology, The University of Tokyo Graduate School of Medicine, Tokyo, Japan

² Biological and Pharmacological Research Laboratories, Central Pharmaceutical Research Institute, Japan Tobacco Inc, Osaka, Japan

and several PHD inhibitors that have been developed as a novel class of HIF-stabilizers and are currently in clinical studies for the treatment of renal anemia.

Clinical trials of PHD inhibitors led to the unexpected discovery of altered glucose and lipid metabolism. In addition to the erythropoietic activity, sustained HIF activation showed pleiotropic effects, such as changes in glucose levels, fat, and cholesterol metabolism [6–9]. For example, roxadustat (FG-4592), which was originally approved for the treatment of anemia in non-dialysis CKD patients and/or hemodialysis (HD) patients [10–12], significantly lowered total cholesterol levels in a dose-dependent manner. Another PHD inhibitor, daprodustat, also lowered low-density lipoprotein (LDL) and high-density lipoprotein (HDL) cholesterol levels in Japanese HD patients [13].

Similar observations have been reported in animal studies [14, 15]. FG-4497 decreased obesity, insulin resistance and reduced liver and white adipose tissue (WAT) weight, adipose size, and the number of inflammation-associated WAT macrophage aggregates in LDL receptor-deficient mice [15]. Matsuura et al. also showed deletion of *Phd2*, the main oxygen sensor, in adipocytes improved diet-induced obesity and associated metabolic abnormalities [16].

The epidemic of obesity and obesity-related diseases, such as dyslipidemia, hypertension, and type 2 diabetes, is rapidly increasing worldwide [17]. The World Health Organization reported in 2014 that more than 1.9 billion adults, 18 years and older, were overweight and of these, over 600 million were obese. Importantly, obesity itself is closely associated with the development of cardiovascular and hepatic diseases [18–20]. Obesity is also a risk factor of CKD. Kidney disease induced by obesity is called obesity-related glomerulopathy (ORG). Kambham et al. analyzed native renal biopsy cases at Columbia University and reported an increase in the prevalence of ORG from 0.2% in 1986–1990 to 2.0% in 1996–2000. In this study, doubling of serum creatinine occurred in 14.3% of ORG and 3.6% culminated in end-stage kidney disease (ESKD) requiring renal replacement therapy during the mean 27 months of follow-up periods [21]. The demographics is retained across ethnic groups.

Major manifestations of ORG are proteinuria, and an increase of glomerular filtration rate (GFR) associated with hemodynamic changes. Renal pathology shows focal segmental glomerulosclerosis (FSGS), glomerulosclerosis, glomerulomegaly with mesangial proliferation, matrix accumulation, and a decreased density of more focally effaced and hypertrophied podocytes with milder foot process fusion [22].

Ingestion of a high-fat diet (HFD) results in weight gain and obesity in rodents [23] and humans [24].

Experimentally, HFD is also associated with development of kidney disease [25], which closely resembles human ORG.

In this study, we hypothesized that HIF activation using a PHD inhibitor, JTZ-951 [26], protects from obesity-related multiple organ pathologies, such as adipose inflammation, hepatic steatosis, and ORG, in mice fed with HFD.

Materials and methods

Animal experiments

C57BL/6J mice were used (CLEA Japan, Inc. Tokyo, Japan). After 1 week of acclimatization, male C57BL/6J mice aged 8 weeks were randomly divided into (1) normal diet (ND; 3590 kcal/kg) ($n = 3$), (2) HFD (5062 kcal/kg, 62.2% kcal fat. [Oriental Yeast, Tokyo, Japan]) ($n = 7$) and (3) HFD with PHD inhibitor, JTZ-951 (provided from Japan Tobacco inc., Osaka, Japan), 0.005% mixed in chow ($n = 7$) groups.

Mice were fed for up to 20 weeks. Body weight (BW) was measured at baseline and every 4 weeks. Mice were housed in metabolic cages for 24 h for collection of urine at 20 weeks. After collecting urine at 20 weeks, mice were euthanized, blood was taken by cardiac puncture, and the kidneys, livers, and epididymal WAT were removed for tissue analyses 6 h after starvation.

The animals were housed in a temperature- and light-controlled environment and were allowed free access to chow and water, unless otherwise indicated. All animal experiments were approved by the ethics committee of the Graduate School of Medicine (P16-011, P16-257), the University of Tokyo, and performed in accordance with the guideline established by the committee.

Histological analyses

Three micrometer formalin-fixed, paraffin-embedded sections were stained with hematoxylin–eosin (HE) (liver and epididymal WAT) or with Periodic Acid-Schiff (PAS) (kidney). Fibrosis in WAT was evaluated with Sirius red staining. ImageJ software was used for quantitative evaluation in each slide. Hepatic steatosis was semi-quantitatively scored as reported previously [27]. Randomly selected fields were scored (0–4) based on the proportion of affected areas, as follows: (0: normal, 1: < 25%, 2: 25–50%, 3: 50–75%, 4: > 75%), and averaged per individual. All evaluation was performed in a blinded manner.

Immunohistochemistry

Either formalin-fixed or methyl-Carnoy's-fixed, paraffin-embedded tissues were sectioned at 3 μm for

immunohistochemistry. The following primary antibodies were used: polyclonal rabbit anti-WT-1 (Wilm's tumor-1, used as a podocyte-specific marker [28]) (1/500, Santa Cruz Biochemistry, Dallas, TX), monoclonal goat anti-type IV collagen (1/800, Southern Biotech, Dallas, TX), rat anti-mouse F4/80 (1/400, Bio-Rad Laboratories, Inc. Hercules, CA), and rabbit IgG anti-HIF-1 α (1/2500, Cayman Chemical, Ann Arbor, MI) for evaluating podocyte injury, mesangial expansion, macrophage infiltration, and HIF-1 α expression. Negative controls included omission of the incubation step with the primary antibody, which yielded no specific staining.

Electron microscopy

Transmission electron microscope (TEM) observation was performed in the kidney cortex. Kidney cortices were promptly cut into 1-mm³ pieces, fixed in 2.5% glutaraldehyde, and diluted 10-fold with 0.1 M phosphate buffer. The sections were examined using a JEM-1011 electron microscope (JEOL, Tokyo, Japan). The kidney block was examined at high magnification ($\times 10,000$). The degree of foot process effacement was measured quantitatively by calculating the percentage of the length of glomerular basement membrane.

Hematocrit measurement

Hematocrit was measured at 4 and 20 weeks. Blood was collected in glass capillary tubes and centrifuged at 12,000 rpm for 6 min. The volume of red blood cells was determined using a hematocrit chart.

Plasma data

Plasma fasting glucose was measured using glucose HK test (Roche-Diagnostics, Basel, Switzerland). Plasma triglyceride (TG) was measured with Determiner L TGII, and total cholesterol (TC) and HDL cholesterol were measured with Determiner L TCII (Kyowa Medex Co. Ltd., Tokyo, Japan). Plasma creatinine was measured using aqua-auto KINOS CRE-III plus (KAINOS Laboratories Inc., Tokyo, Japan). Plasma adiponectin was measured with Mouse/Rat adiponectin ELISA kit (Otsuka Pharmaceutical Co. Ltd., Tokyo, Japan). Plasma aspartate aminotransferase (AST) and alanine aminotransferase (ALT) were measured with GOT IFCC and GPT IFCC kit (Roche-Diagnostics, Basel, Switzerland). Plasma erythropoietin concentration was measured with Immunoelit EPO (Toyobo Co. Ltd., Osaka, Japan).

ELISA for albumin creatinine ratio

To measure urinary albumin creatinine ratio (ACR), mouse albumin ELISA quantitation Set (Bethyl Laboratoeis,

Montgomery, TX) and creatinine kit (Wako, Osaka, Japan) were used.

Real-time PCR analysis

RNA was isolated using RNAiso Plus (Takara, Shiga, Japan) and reverse-transcribed with PrimeScript RT Master Mix (Perfect Real Time, Takara, Shiga, Japan), according to the supplier's protocol. One-twentieth (vol/vol) of the synthesized cDNA was used as a template for PCR quantification. PCR was performed on CFX96 (Bio-rad, Hercules, CA) with the THUNDERBIRD SYBR qPCR mix (Toyobo, Osaka, Japan). Data were analyzed using the $2^{-\Delta\Delta C_t}$ method. Relative expression levels were calculated using β -actin mRNA as a reference. Primers for quantification are shown in Table 1.

In vitro studies

The possible effect of PHD inhibitors on macrophage polarization was tested in RAW264.7 cells (RIKEN BRC, Ibaraki, Japan). Cells were grown in DMEM, high glucose (Nissui Seiyaku, Tokyo, Japan) supplemented with 10% FBS. Cells grown on poly-L-lysine-coated culture plates were treated with either the vehicle, 100 ng/ml interferon-gamma (IFN- γ) (PeproTech Inc., Rocky Hill, NJ), or 20 ng/ml interleukin (IL)-4 (PeproTech Inc., Rocky Hill, NJ), with or without 10 μ M JTZ-951. After 24 h of stimulation, cells were harvested and subjected to mRNA quantification of representative M1 and M2 macrophage markers.

Statistics

The results were given as means \pm SD. Two-sided student's unpaired *t* test, Welch's *t* test, and Mann-Whitney's U test were used for the data for two groups. Statistical differences in multiple groups were analyzed by multivariate analysis of variance (MANOVA), Tukey-Kramer test, and Steel-Dwass test. Differences with *P*-values of < 0.05 were considered statistically significant. Analyses were performed with JMP 13[®] software (SAS Institute Inc., Cary, NC).

Results

HIF stabilization by PHD inhibition in mice

JTZ-951 is a PHD inhibitor that is currently in phase 3 clinical trial for the treatment of renal anemia in Japan.

In a pilot study, HIF activation was confirmed by HIF-1 α immunohistochemistry in the kidney and liver. In the kidney, HIF-1 α was stained in the nuclei of glomerular and tubular epithelial cells in the HFD + JTZ-951 group,

Table 1 A list of primers

Target genes	Forward (sequence 5' → 3')	Reverse (sequence 5' → 3')
<i>β-actin</i>	5'-CTTTCTACAATGAGCTGCGTG-3'	5'-TCATGAGGTAGTCTGTCAGG-3'
<i>EPO</i>	5'-GAGGCAGAAAATGTCACGATG-3'	5'-CTTCCACCTCCATTCCTTTTCC-3'
<i>SLC2A1</i>	5'-GTGACGATCTGAGCTACGGG-3'	5'-ACTCCTCAATAACCTTCTGGGG-3'
<i>PGK1</i>	5'-GGAGCGGGTCGTGATGA-3'	5'-GCCTTGATCCTTTGGTTGTTTG-3'
<i>TNF-α</i>	5'-CATCTTCTCAAAATTCGAGTGACAA-3'	5'-TGGGAGTAGACAAGGTACAACCC-3'
<i>IL-6</i>	5'-CCAGTTGCCTTCTTGGGACT-3'	5'-GGTCTGTTGGGAGTGGTATCC-3'
<i>MCP-1</i>	5'-ACTGAAGCCAGCTCTCTCTCCTC-3'	5'-TTCCTTCTTGGGGTCAGCACAGAC-3'
<i>RANTES</i>	5'-CCTCACCATATGGCTCGGAC-3'	5'-ACGACTGCAAGATTGGAGCA-3'
<i>CCR-2</i>	5'-TCAGCTGCCTGCAAAGACCAG-3'	5'-CATACGGTGTGGTGGCCCT-3'
<i>CCR-5</i>	5'-AACTCTGGCTCTGCAGGATGGA-3'	5'-GAGATGGCCAGGTTGAACAGGT-3'
<i>adiponectin</i>	5'-GTCAGTGGATCTGACGACACCAA-3'	5'-ATGCCTGCCATCCAACCTG-3'

Erythropoietin (EPO), *solute carrier family 2 member 1 (SLC2A1)* and *phosphoglycerate kinase 1 (PGK1)* were used as HIF target genes. *Tumor necrosis factor-α (TNF-α)*, *interleukin (IL)-6*, *monocyte chemoattractant protein (MCP)-1*, *regulated on activation normal T cell expressed and secreted (RANTES)*, *chemokine (C-C motif) receptor 2 (CCR-2)*, and *chemokine (C-C motif) receptor 5 (CCR-5)* were used as inflammation markers. *Adiponectin* was quantified in WAT.

whereas there was no positive staining in the HFD group (Fig. 1a). Accumulation of HIF-1 α was observed in tubules of both the cortex and medulla. The expression was marked in distal convoluted tubules and collecting ducts, but was evident in all tubular segments, confirming successful activation of HIF with this method. In the liver, HIF-1 α was stained in hepatocytes of the HFD + JTZ-951 group, whereas there was no positive staining in the HFD group (Fig. 1a). Activation of HIF in WAT was confirmed by quantifying mRNA expression of HIF target genes. Relative mRNA expression of *SLC2A1* and *PGK1* was significantly increased by JTZ-951 in WAT (Fig. 1b).

To additionally demonstrate activation of HIF in our model, hematocrit levels were measured at 4 and 20 weeks (Fig. 1c). Hematocrit levels were significantly higher after 4 weeks (early phase), but the difference was not statistically significant at 20 weeks. A transient rise in hematocrit levels is likely accounted for by the administered amount of JTZ-951 corrected for body weight, which was higher at 4 weeks than at 20 weeks. In keeping with this, plasma erythropoietin concentration, renal and hepatic *EPO* mRNA did not differ significantly between treatment groups at 20 weeks (Fig. 1d, e).

JTZ-951 improved obesity

Next, we investigated the possible impact of JTZ-951 on obesity, hyperlipidemia, and obesity-related diseases including ORG, using C57BL/6J mice fed with HFD [29, 30].

The weight of mice at baseline was almost the same among three groups, but mice became obese in the HFD and HFD + JTZ-951 groups, as compared with those in the ND group, which became apparent from 4 weeks after

intervention (Fig. 2a) and this tendency continued until the end. BW in the HFD + JTZ-951 group was smaller than that in the HFD group, which became significant from week 4 onwards. Notably, the average amount of food intake in the HFD + JTZ-951 group was significantly larger than that in the HFD group (Fig. 2b; HFD 3.1 g/day vs. HFD + JTZ-951 3.8 g/day, $P = 0.021$).

JTZ-951 improved plasma non-HDL-cholesterol levels

Plasma glucose, triglyceride (TG), total cholesterol (TC), high-density lipoprotein cholesterol (HDL-c), non-HDL cholesterol (nHDL-c), creatinine, aspartate aminotransferase (AST), alanine aminotransferase (ALT), and adiponectin were measured at the end of the experiment, after 6 h of starvation period (Table 2). No significant difference in plasma glucose levels was observed among three groups. HFD feeding significantly increased plasma TC and HDL-c levels, whereas JTZ-951 treatment did not significantly influence these levels. On the other hand, JTZ-951 reduced nHDL-c levels significantly, as compared with the HFD group. Plasma adiponectin levels were not significantly different among three groups.

JTZ-951 reduced the number of macrophages infiltrating white adipose tissue (WAT), without significant effects on epididymal WAT weight and adipocyte size

Obesity is associated with an increase in WAT weight (adipocyte enlargement), which is mechanistically linked to chronic adipose tissue inflammation [31–33]. HFD

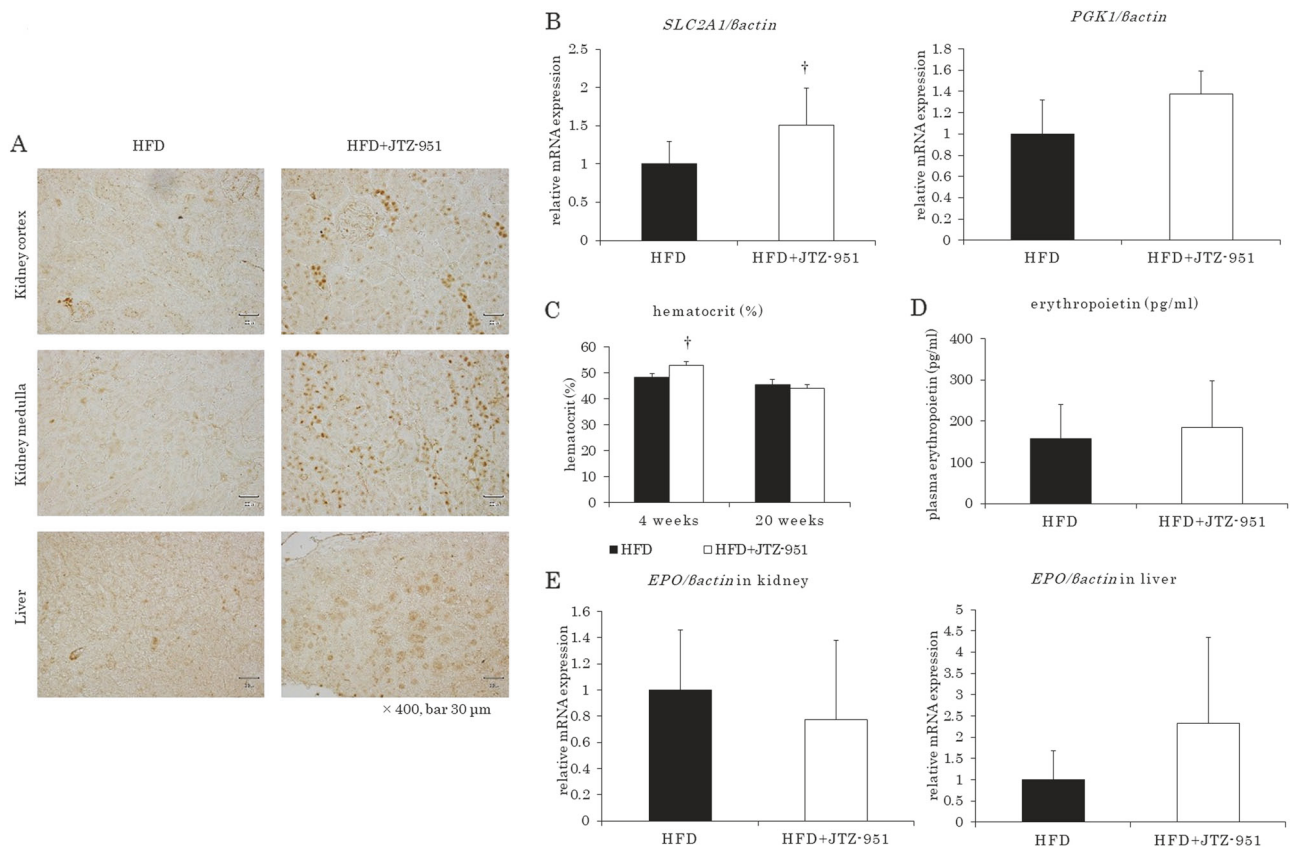


Fig. 1 HIF expression after treatment with PHD inhibitors in mice. **a** HIF-1 α expression in kidneys and livers of mice. In the high-fat diet (HFD) + JTZ-951 group, nuclear staining was observed in tubular epithelial cells both in the cortex and medulla and in hepatocytes, whereas in the HFD group, there was no specific staining ($\times 400$, bars = 30 μ m). **b** Relative mRNA expression of *solute carrier family 2 member 1* (*SLC2A1*) and *phosphoglycerate kinase 1* (*PGK1*) in WAT. Data are shown as means \pm SD. Unpaired two-sided *t* test. [†] $P < 0.05$ compared with HFD group. (HFD, $n = 7$; HFD + JTZ-951, $n = 7$). **c**

Hematocrit levels at 4 and 20 weeks. Data are shown as means \pm SD. Unpaired two-sided *t* test. [†] $P < 0.05$ compared with HFD group (HFD, $n = 7$; HFD + JTZ-951, $n = 7$). **d** Plasma erythropoietin levels. Data are shown as means \pm SD. Unpaired two-sided *t* test (HFD, $n = 7$; HFD + JTZ-951, $n = 7$). **e** *Erythropoietin* (*EPO*) mRNA expression in kidneys and livers at 20 weeks. Data are shown as means \pm SD. Unpaired two-sided *t* test [kidney] and Mann–Whitney’s U test [liver] (HFD, $n = 7$; HFD + JTZ-951, $n = 7$)

increased epididymal WAT weight, but it did not change between HFD and HFD + JTZ-951 groups (Fig. 3a), which was consistent after adjustment for BW (Fig. 3b). Adipocyte areas were also enlarged by HFD, whereas JTZ-951 did not significantly change these parameters (Fig. 3c, d). On the other hand, HFD facilitated macrophage infiltration to adipocytes and the number of crown-like structures (CLS) significantly increased, whereas JTZ-951 offset these changes (Fig. 3c, e). HFD also induced fibrosis in WAT, which was improved by JTZ-951 (Fig. 3c, f). There was a strong correlation between the number of CLS and the degree of fibrosis (Fig. 3g). In addition, relative mRNA expression of inflammatory markers was quantified. Several of the markers, such as *TNF- α* , *MCP-1*, and *CCR-5*, were significantly increased by HFD, whereas JTZ-951 treatment only canceled an increase in *TNF- α* mRNA (Fig. 3h).

Relative mRNA expression of *adiponectin* was significantly smaller in the HFD group, and JTZ-951 treatment significantly increased mRNA expression of *adiponectin* (Fig. 3h).

To test for the potential impact of PHD inhibitors on macrophage polarization, we stimulated RAW264.7 cells with JTZ-951, under non-polarized, M1-polarized (IFN- γ), or M2-polarized (IL-4) conditions (Fig. 4). In non-polarized conditions, JTZ-951 induced *iNOS* and *arginase* mRNA, whereas in IFN- γ -treated conditions, it significantly suppressed *TNF- α* mRNA and increased *iNOS* and *CD163* mRNA. In IL-4-treated conditions, on the other hand, JTZ-951 did not significantly change the expression of all M1 and M2 markers tested. These results imply that PHD inhibition by JTZ-951 does not significantly influence polarization of macrophages in a cell-autonomous manner.

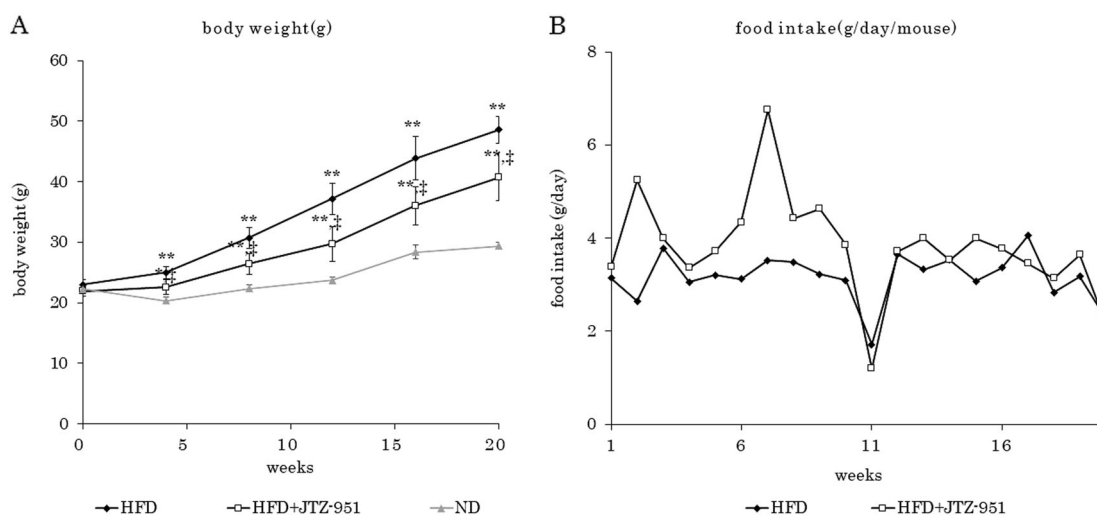


Fig. 2 Changes in body weight and food intake. **a** Body weight (BW) was measured at baseline and every 4 weeks. Data are shown as means \pm SD. Multivariate analysis of variance (MANOVA). * $P < 0.05$ compared with the normal diet (ND) group. ** $P < 0.01$ compared with

the ND group. $\ddagger P < 0.01$ compared with the HFD group (HFD, $n = 7$; HFD + JTZ-951, $n = 7$; normal diet [ND], $n = 3$). **b** Time-course changes in food intake from baseline to 20 weeks. The amount of food intake was calculated every week

JTZ-951 improved hepatic steatosis

Hepatic steatosis is an underlying feature of nonalcoholic fatty liver disease, which is the most common form of liver disease and is present in up to 70% of obese individuals [34]. Hepatic steatosis is characterized by macro and micro vesicles of fat, predominately triglycerides, accumulate within hepatocytes [35].

In our study, HFD caused hepatic steatosis in mice (Fig. 5a). Semi-quantitative evaluation of hepatic steatosis revealed significant improvement by JTZ-951 treatment (Fig. 5b). Real-time PCR showed that mRNA expression of *MCP-1*, *CCR-2*, *RANTES*, and *CCR-5* was significantly induced by HFD, whereas JTZ-951 treatment canceled an increase in *MCP-1* mRNA. Albeit not significant, quantification of additional inflammation markers, such as *IL-6*, *TNF- α* , and *CCR-2*, showed similar tendency (Fig. 5c). Liver injury was evaluated by measuring plasma AST and ALT levels. HFD induced non-significant increases in AST and ALT levels, which tended to be smaller in the HFD + JTZ-951 group, although they were not significant, likely reflecting inherent variability of the model (Table 2).

JTZ-951 reduced albuminuria, glomerular macrophage infiltration, and mesangial expansion

ORG induces albuminuria, glomerulomegaly, mesangial expansion, and focal segmental glomerulosclerosis (FSGS). In this study, HFD increased levels of urinary albumin creatinine ratio (ACR) at 20 weeks, which were significantly smaller in the HFD + JTZ-951 group

(Fig. 6a). In histological evaluation, HFD tended to induce glomerulomegaly (HFD vs. ND, $P = 0.0677$), but JTZ-951 treatment did not improve glomerular tuft area compared with the HFD group (Fig. 6b, c). On the other hand, type IV collagen-positive areas were significantly smaller by JTZ-951 treatment, suggesting that JTZ-951 improved mesangial expansion induced by HFD (Fig. 6b, d). In addition, the number of F4/80-positive macrophages in the glomeruli was also smaller in the HFD + JTZ-951 group, suggesting that JTZ-951 reduced macrophage infiltration into the glomeruli (Fig. 6b, e).

Loss of glomerular podocytes, as well as structural derangement of foot processes, has been implicated in the development of albuminuria, which we evaluated further. Although HFD did not reduce the number of WT-1-positive podocytes (Fig. 6b, f), podocyte foot process effacement was clearly observed by electron microscopy, compared with the ND group (Fig. 7a, b). JTZ-951 treatment did not significantly improve the extent of foot process effacement (Fig. 7a, b). In this model, a non-significant tendency was observed between the level of ACR and the extent of foot process effacement, suggesting that additional factors other than foot process effacement might contribute to the development of albuminuria (Fig. 7c).

Kidney injury was evaluated by measuring plasma creatinine levels. Plasma creatinine level tended to be higher in both HFD-treated groups (HFD vs ND, $P = 0.10$; HFD + JTZ-951 vs. ND, $P = 0.077$), but JTZ-951 treatment had no recognizable effects on plasma creatinine levels (Table 2).

Table 2 Laboratory data

	Glucose (mg/dL)	TG (mg/dL)	TC (mg/dL)	HDL-c (mg/dL)	nHDL-c (mg/dL)	Creatinine (mg/dL)	AST (IU/L)	ALT (IU/L)	Adiponectin (μ g/mL)
HFD	252.8 \pm 23.3	14.8 \pm 5.0	202.3 \pm 14.8 ^a	186.8 \pm 11.6 ^a	15.5 \pm 4.8	0.074 \pm 0.030	280.4 \pm 159.8	146.4 \pm 90.2	18.2 \pm 3.6
HFD + JTZ-951	253.1 \pm 50.4	16.4 \pm 6.1	179.9 \pm 29.9 ^a	172.5 \pm 31.4 ^a	7.4 \pm 5.1 ^b	0.077 \pm 0.020	165.6 \pm 73.1	62.8 \pm 57.8	17.5 \pm 2.2
ND	216.3 \pm 20.8	20.9 \pm 10.0	97.1 \pm 7.7	84.8 \pm 6.6	12.3 \pm 2.7	0.033 \pm 0.020	167.7 \pm 74.4	25.2 \pm 0.6	13.2 \pm 1.1

Plasma glucose, triglyceride (TG), total cholesterol (TC), HDL cholesterol (HDL-c), non-HDL cholesterol (nHDL-c), creatinine, aspartate aminotransferase (AST), alanine aminotransferase (ALT), and adiponectin were measured and expressed as mean \pm SD

^a $P < 0.01$ compared with ND group

^b $P < 0.05$ compared with HFD group (HFD, $n = 7$; HFD + JTZ-951, $n = 7$; ND, $n = 3$)

mRNA expression of *adiponectin* negatively correlated with BW, hepatic steatosis, and ACR

It has been reported that plasma adiponectin levels negatively correlate with BW and ACR. In CKD, however, plasma adiponectin levels are higher due to disturbances in renal biodegradation and elimination [36]. Therefore, these associations may be variable. In this regard, we evaluated the correlation between mRNA expression of *adiponectin* and BW, hepatic steatosis and ACR (Fig. 8a–c). *Adiponectin* mRNA expression was inversely correlated with BW (Fig. 8a), scores of hepatic steatosis (Fig. 8b), and ACR at 20 weeks (Fig. 8c).

On the other hand, plasma adiponectin levels, which were higher in the HFD and HFD + JTZ-951 groups compared with the ND group (Table 2), did not correlate with these parameters (Fig. 8d–f).

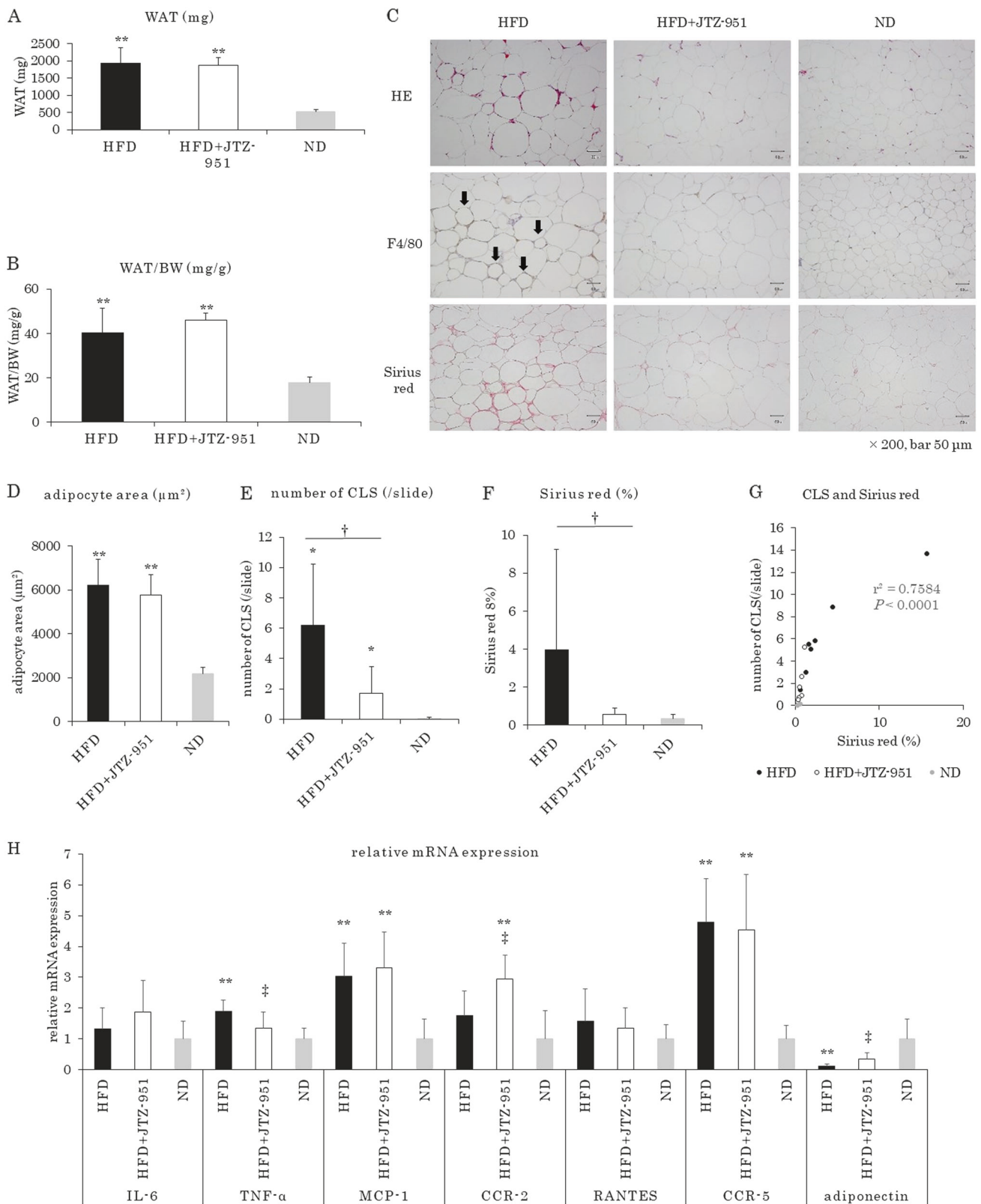
Discussion

The present study highlights the net systemic effect of a PHD inhibitor, JTZ-951, on obesity and associated multiple organ pathology, such as WAT inflammation, hepatic steatosis, and glomerular injury, toward protection.

Obesity causes an increase in WAT weight by adipocyte enlargement, which is associated with chronic inflammation in adipose tissue [31–33]. Previous reports showed that PHD inhibition reduced not only BW but also WAT growth [15, 16, 27]. In this study, however, obesity induced by HFD was significantly improved by JTZ-951 treatment, but the weight and the area of epididymal WAT did not significantly decrease, even after adjustment for BW. The effect of JTZ-951 treatment on epididymal WAT was observed in the reduction of the number of CLS.

Obesity causes an increase in WAT weight, but it seems to reach a plateau at an earlier time point as compared with other parameters. Strissel et al. showed that adipose size and epididymal WAT weight of HFD fed mice were the highest at 12 weeks, which then began to decrease. This was in contrast to changes in liver weight that started to increase after the epididymal WAT growth completed [37]. Therefore, although we were unable to observe decreases in the weight and the area of epididymal WAT at 20 weeks by JTZ-951 treatment, measurement at an earlier time point might have revealed an effect. In addition, adipocyte area is significantly greater in the subcutaneous depots than in the visceral fat, both in *db/db* and *ob/ob* obese mice, suggesting a differing sensitivity to HFD [38]. Therefore, there is also a possibility that measurement of other visceral or subcutaneous fats might have revealed a reduction by JTZ-951.

CLS is defined as a cluster of macrophages which are localized at the periphery of exclusively dead adipocytes. In



these lesions, macrophages phagocytize and process adipocytes [39]. In obese WAT, adipocyte hypertrophy becomes apparent and dead adipocytes increase together

with a higher frequency of CLS, suggesting that adipocyte death is one driver of the infiltration of macrophages [37]. Maruno et al. showed the correlation between mean

◀ **Fig. 3** The effect of JTZ-951 on epididymal white adipose tissue of mice with HFD. **a** Weight of white adipose tissue (WAT). Data are shown as means \pm SD, Tukey–Kramer test. $**P < 0.01$ compared with the ND group (HFD, $n = 7$; HFD + JTZ-951, $n = 7$; ND, $n = 3$). **b** WAT weight adjusted for BW. Data are shown as means \pm SD, Tukey–Kramer test. $**P < 0.01$ compared with ND group (HFD, $n = 7$; HFD + JTZ-951, $n = 7$; ND, $n = 3$). **c** HE staining, F4/80 and Sirius red staining of WAT in the HFD, HFD + JTZ-951 and ND groups. Arrows in F4/80 staining showed crown-like structure (CLS) in the HFD group ($\times 200$, bars = 50 μm). **d** Adipocyte size in the HFD, HFD + JTZ-951 and ND groups. Data are shown as means \pm SD, Tukey–Kramer test. $**P < 0.01$ compared with the ND group (HFD, $n = 7$; HFD + JTZ-951, $n = 7$; ND, $n = 3$). **e** Number of CLS per slide in HFD, HFD + JTZ-951 and ND groups. Data are shown as means \pm SD, Tukey–Kramer test. $^{\dagger}P < 0.05$ compared with the HFD group (HFD, $n = 7$; HFD + JTZ-951, $n = 7$; ND, $n = 3$). **f** The area of Sirius red-positive staining (%) in the HFD, HFD + JTZ-951 and ND groups. Data are shown as means \pm SD, Tukey–Kramer test. $^{\dagger}P < 0.05$ compared with the HFD group (HFD, $n = 7$; HFD + JTZ-951, $n = 7$; ND, $n = 3$). **g** The relationship between the number of CLS (/slide) and the degree of fibrosis by Sirius red staining (%) (HFD, $n = 7$; HFD + JTZ-951, $n = 7$; ND, $n = 3$). **h** Relative mRNA expression of inflammatory markers and *adiponectin*. Relative mRNA expression of inflammatory markers, such as *interleukin (IL)-6*, *tumor necrosis factor- α (TNF- α)*, *monocyte chemoattractant protein (MCP)-1*, *chemokine (C-C motif) receptor 2 (CCR-2)*, *regulated on activation normal T cell expressed and secreted (RANTES)* and *chemokine (C-C motif) receptor 5 (CCR-5)*, were quantified in WAT of the HFD, HFD + JTZ-951, and ND groups. Similarly, relative mRNA expression of *adiponectin* was quantitatively evaluated. Data are shown as means \pm SD, Tukey–Kramer test was used except for *adiponectin* (Steel–Dwass test). $*P < 0.05$ compared with the ND group. $**P < 0.01$ compared with the ND group. $^{\ddagger}P < 0.01$ compared with the HFD group (HFD, $n = 7$; HFD + JTZ-951, $n = 7$; ND, $n = 3$)

adipocyte areas and CLS density in visceral depots [38]. In this study, the number of CLS increased by HFD, which was significantly reduced by JTZ-951. These changes correlated with the extent of adipocyte interstitial fibrosis, to be consistent with a previous report [40].

Macrophages infiltrating into WAT promote obesity-induced inflammation. These macrophages secrete inflammatory mediators, such as TNF- α , IL-6, and MCP-1, which are elevated in WAT in obese mice and humans [41, 42]. Our results showed that HFD upregulated adipocyte mRNA expression of these inflammatory markers except for IL-6, and JTZ-951 treatment canceled the upregulation of adipocyte mRNA expression of TNF- α in mice on an HFD. Lack of hepatic IL-6 mRNA induction in our study may be accounted for by the transient induction at earlier time point (week 16) as compared with persistent upregulation of TNF- α and MCP-1 at later stages (week 20) [37].

Preceding studies report on multifactorial roles of HIF on adipocyte growth, obesity, and insulin resistance. On the one hand, HIF-1 suppresses white adipocyte oxidative metabolism and leads to white adipose accumulation, inflammation, and insulin resistance, which was demonstrated in adipocyte-specific *HIF-1 β* or *HIF-1 α* knockout

mice [43, 44]. On the other hand, mice with systemic HIF activation by pharmacological PHD inhibitor, FG-4497, and *Phd2* hypomorphic mice showed reductions in white adipose weight, adipocyte area, and macrophage infiltration [27]. In addition, adipocyte-specific *Phd2* knockout mice similarly reduced body weight, adipocyte area, and macrophage infiltration [16]. The results of our study clearly indicate an anti-obesity effect of systemic PHD inhibition, and we surmise that JTZ-951 induced other HIF-dependent or independent events that have possibly overridden the pro-obesity effect of HIF-1 in white adipocytes.

The protective effect of JTZ-951 on fatty changes of the liver is consistent with previous studies [27]. Hepatic steatosis induced by HFD was significantly ameliorated by JTZ-951 treatment, which was associated with a decreasing tendency of plasma AST and ALT levels. Relative mRNA expression of inflammatory markers also tended to decrease by JTZ-951 treatment, though all inflammatory markers did not reach statistical significance, except for *MCP-1*.

Although HFD for 20 weeks induced hepatic steatosis and an increase of mRNA expression of many of inflammatory markers, HFD did not significantly induce mRNA expression of IL-6 and TNF- α in our study. However, lack of the induction of these cytokines should be interpreted within the following current understandings. TNF- α has a role in developing hepatic steatosis. But some studies suggested that hepatic steatosis was not dependent on TNF- α [45, 46]. In addition, the contribution of IL-6 in obesity-induced inflammation is multidirectional, and some studies showed hepatoprotective and hepatoproliferative effects of IL-6 upon injury [47, 48].

Preceding studies demonstrated that the stabilization of HIF-2 α upregulated insulin receptor substrate 2 (*Irs2*), thereby repressing sterol regulatory element-binding protein 1c (*Srebp1c*) and fatty acid synthase (*Fas*) [49, 50]. In our study, however, *Srebp1c*, *Fas*, and *Irs2* mRNA expression did not differ significantly irrespective of JTZ-951 treatment (data not shown). Notably, mRNA expression of *adiponectin* was upregulated by JTZ-951, which was paralleled by improvement in obesity. Adiponectin, one of the most abundant and adipose tissue-specific adipokines, has an anti-steatotic effect on the hepatocytes, because of an increase of free fatty acid oxidation and a decrease of gluconeogenesis, free fatty acid influx and de novo lipogenesis [51]. Adiponectin also has anti-inflammatory and anti-fibrotic effects. Its anti-inflammatory effect is mainly achieved by suppressing inflammatory mediators, such as TNF- α and IL-6, and inducing anti-inflammatory mediators.

Some studies suggested a predictive role of hypoadiponectinaemia in hepatic steatosis [52, 53]. In addition, a systematic review showed a direct association between an increase in adiponectin levels by thiazolidinediones treatment and hepatic histological improvement [54]. These

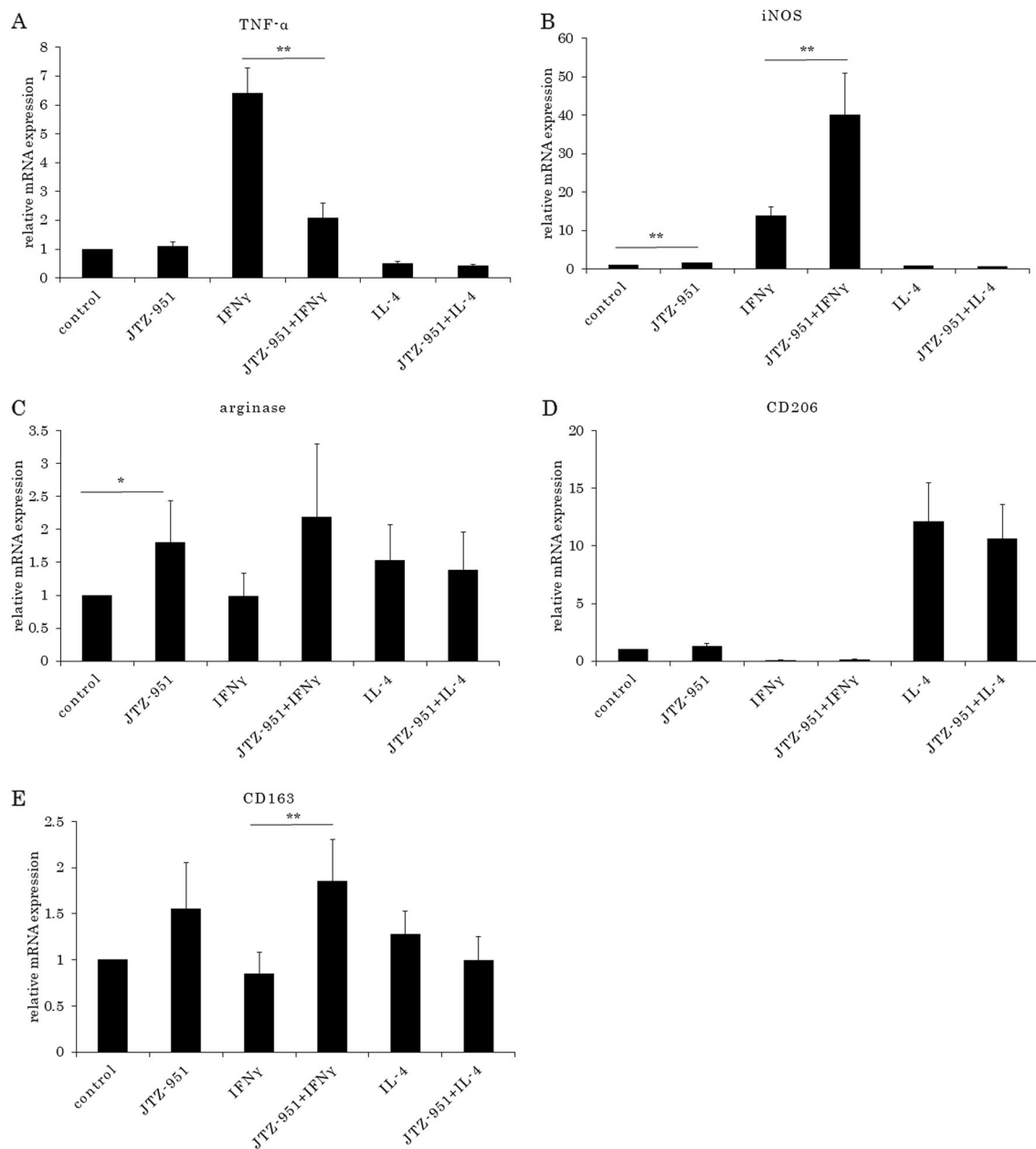


Fig. 4 The impact of JTZ-951 on macrophage polarization. The potential impact of PHD inhibitors on macrophage polarization was tested in RAW264.7 cells. Both M1 (TNF- α , iNOS) and M2 (arginase, CD206, CD163) markers were quantitatively evaluated in non-

polarized, M1-polarized (IFN- γ -treated), and M2-polarized (IL-4-treated) conditions, in the presence or absence of JTZ-951. Data are shown as means \pm SD, Unpaired two-sided *t* test. **P* < 0.05; ***P* < 0.01, respectively. *n* = 4)

results support that there is an additional pathway to improve hepatic steatosis through an increase of mRNA expression of *adiponectin* in WAT.

In the kidney, JTZ-951 treatment reduced levels of ACR at 20 weeks. Glomerular tuft area became larger by HFD, albeit not statistically significant because of a limited number of animals in the ND group (HFD vs. ND groups, *P* = 0.0677). In addition, mesangial expansion by type IV collagen and macrophage infiltration into the glomeruli by F4/80 also tended to increase by HFD, though there was no

statistical significance because of a limited number of ND-fed mice. But, significant decreases of mesangial expansion and macrophage infiltration into the glomeruli were observed by JTZ-951 treatment in mice with a HFD. These results suggest that JTZ-951 treatment caused the structural and functional changes in the kidney and resulted in reduction of level of ACR.

HIF has an important role in inflammatory responses mediated by neutrophils and macrophages. However, it influences multidirectional pathogenic pathways and the net

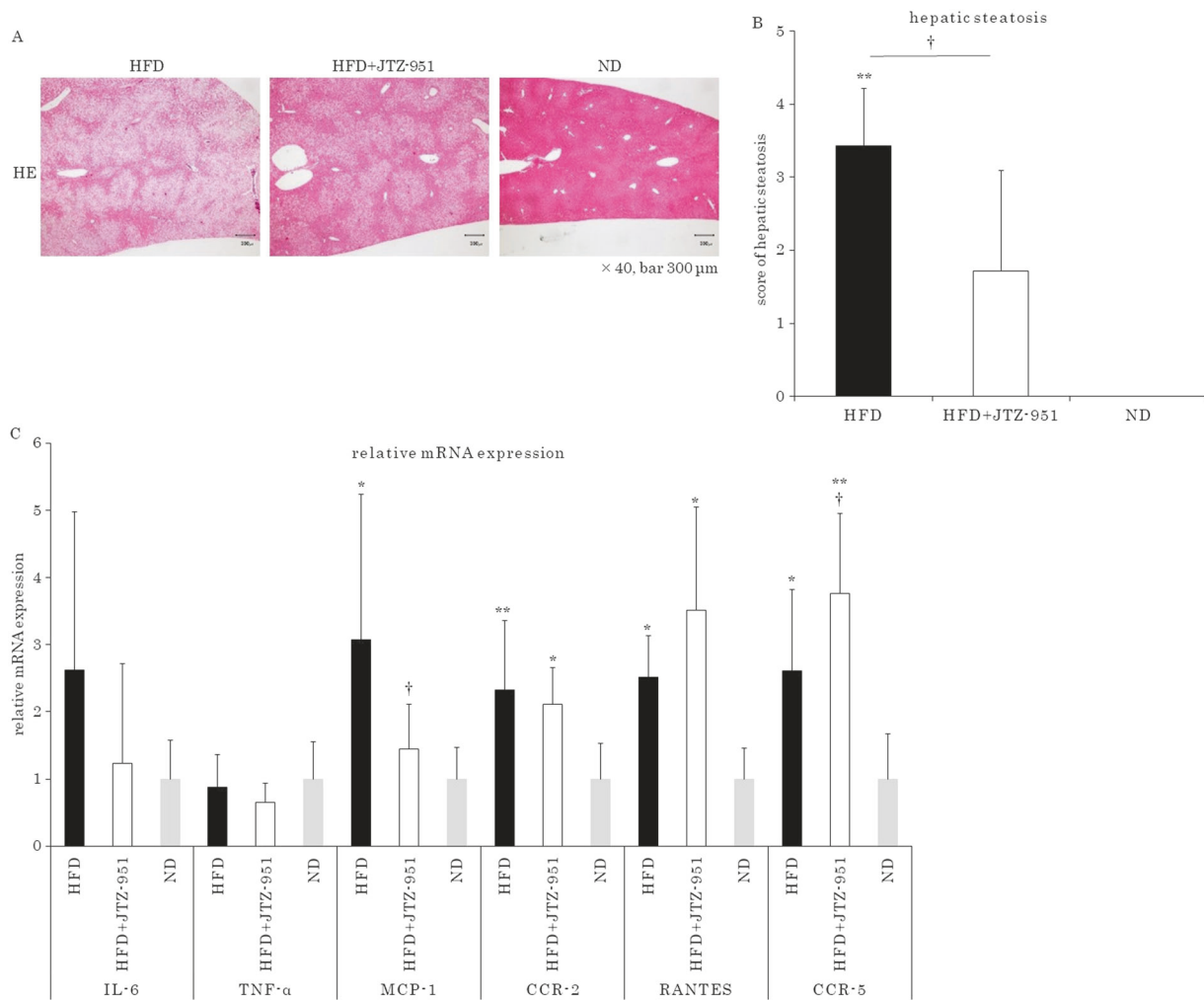


Fig. 5 The effect of JTZ-951 on the livers of mice fed a HFD. **a** HE staining of the liver in HFD, HFD + JTZ-951, and ND groups ($\times 40$, bars = 300 μm). **b** Scoring of hepatic steatosis in the HFD, HFD + JTZ-951, and ND groups. Data are shown as means \pm SD, Tukey–Kramer test. $**P < 0.01$ compared with ND group. $^\dagger P < 0.05$ compared with the HFD group (HFD, $n = 7$; HFD + JTZ-951, $n = 7$; ND, $n = 3$).

c Relative mRNA expression of inflammatory markers. mRNA for *IL-6*, *TNF- α* , *MCP-1*, *CCR-2*, *RANTES*, and *CCR-5* were quantitatively evaluated. Data are shown as means \pm SD, Tukey–Kramer test. $*P < 0.05$ compared with the ND group. $**P < 0.01$ compared with the ND group. $^\dagger P < 0.05$ compared with the HFD group (HFD, $n = 7$; HFD + JTZ-951, $n = 7$; ND, $n = 3$).

effects appear to depend on the pathological context. Some studies reported that *Phd2* inhibition resulted in an exaggerated inflammatory response associated with higher neutrophil motility [55], and HIF activation facilitated macrophage migration via metabolic shift toward glycolysis [56]. On the other hand, macrophage infiltration into WAT was significantly suppressed by PHD inhibition in animal obesity models, irrespective of improvement in obesity [15, 16], suggesting that PHD inhibition act to reduce macrophage infiltration in the context of obesity. In addition, myeloid-specific deletion of *Hif-1 α* was sufficient to promote inflammation in the mouse model of tubulointerstitial fibrosis [57]. These findings are in keeping with the anti-inflammatory role of PHD inhibition as observed in this

study. In addition to glomerular inflammation, oxidative stress is also a candidate driver for the development of albuminuria. However, levels of urinary 2-thiobarbituric acid reactive substances (TBARS) did not differ between the HFD and HFD + JTZ-951 groups (HFD 0.32 vs. HFD + JTZ-951 0.48 $\mu\text{mol/mgCr}$, $P = 0.20$), which makes it less likely as a major factor accounting for the reduction of albuminuria.

Podocytes form complicated foot process within the glomerulus, whose specialized touches wrap up glomerular capillaries shaping the slit diaphragms that protect large proteins from entering the urine. Selective injury to podocytes can lead to primary kidney diseases, for example, FSGS with podocyte loss [58, 59]. Podocyte loss is

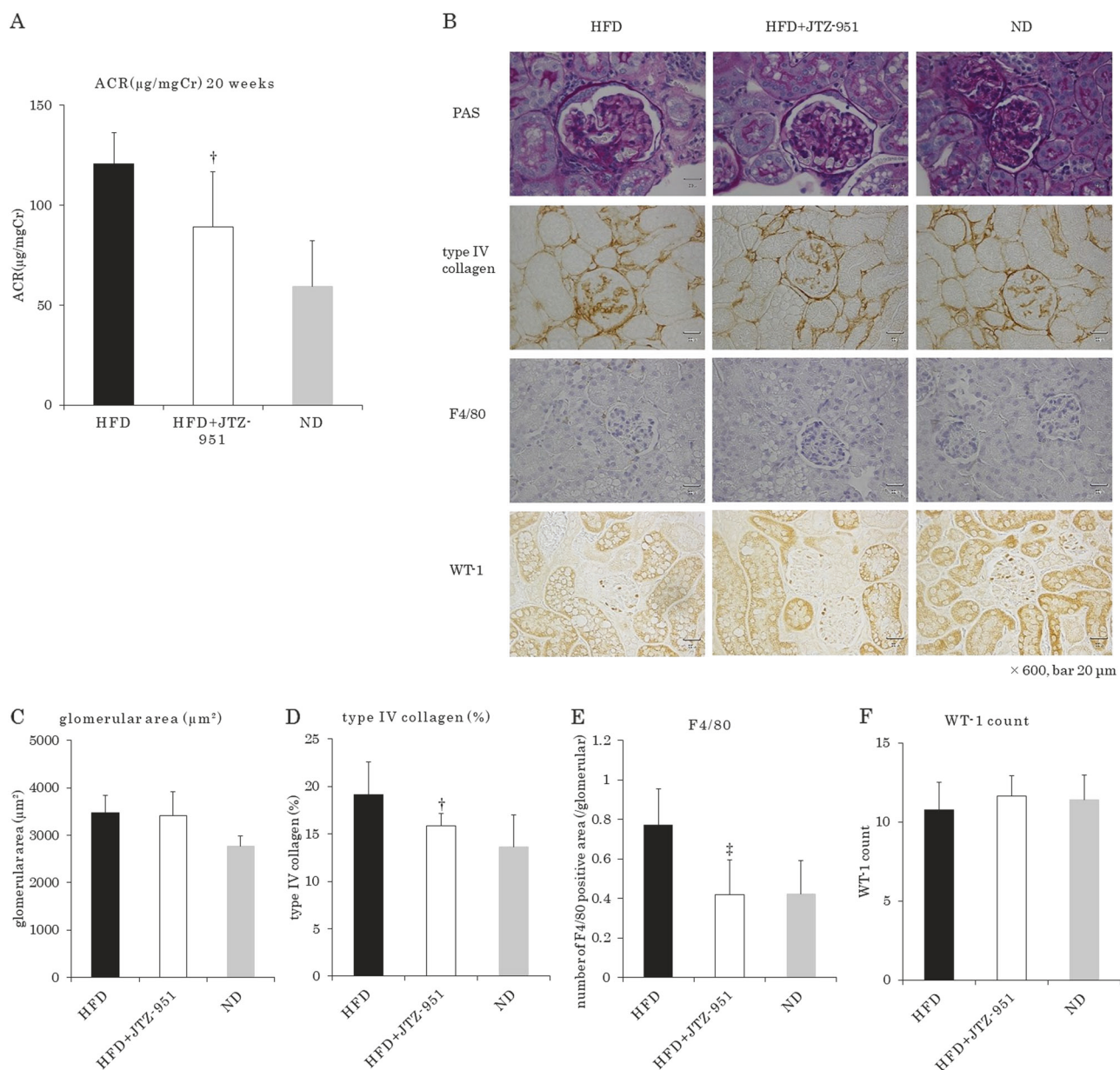


Fig. 6 The effects of JTZ-951 on obesity-related kidney injury. **a** Albumin creatinine ratio (ACR) was measured at 20 weeks. Note that one mouse in the HFD group escaped ACR quantification because of the insufficient amount of urine collection. Data are shown as means \pm SD, Unpaired two-sided *t* test was used between the HFD and HFD + JTZ-951 groups. [†] $P < 0.05$ compared with the HFD group (HFD, $n = 6$; HFD + JTZ-951, $n = 7$; ND, $n = 3$). **b** PAS staining, immunohistochemistry of type IV collagen, F4/80, and WT-1 (Wilm's tumor-1) staining of the kidney in the HFD, HFD + JTZ-951, and ND groups ($\times 600$, bars = 20 μm). **c** Glomerular tuft area was measured using by ImageJ. Data are shown as means \pm SD (HFD, $n = 7$; HFD + JTZ-951,

$n = 7$; ND, $n = 3$). **d** Quantification of type IV collagen in the glomeruli. Data are shown as means \pm SD, Welch's *t* test was used between the HFD and HFD + JTZ-951 groups. [†] $P < 0.05$ compared with HFD group (HFD, $n = 6$; HFD + JTZ-951, $n = 7$; ND, $n = 3$). **e** Quantification of infiltrating macrophages in the glomeruli. Data are shown as means \pm SD, Unpaired two-sided *t* test was used between the HFD and HFD + JTZ-951 groups. ^{††} $P < 0.01$ compared with the HFD group. (HFD, $n = 7$; HFD + JTZ-951, $n = 7$; ND, $n = 3$). **f** Quantification of the podocyte number by WT-1 counts. Data are shown as means \pm SD. (HFD, $n = 7$; HFD + JTZ-951, $n = 7$; ND, $n = 3$)

similarly observed in systemic diseases, such as diabetic kidney disease [60], obesity, and the metabolic syndrome [61], which leads to the formation of sclerosing areas and possibly accounts for CKD progression [62]. In this study, JTZ-951 treatment did not significantly improve the degree

of foot process effacement, suggesting that JTZ-951 treatment reduced albuminuria by acting on other components and pathways of injury.

Interestingly, this study also showed a negative correlation between relative mRNA expression of *adiponectin* in

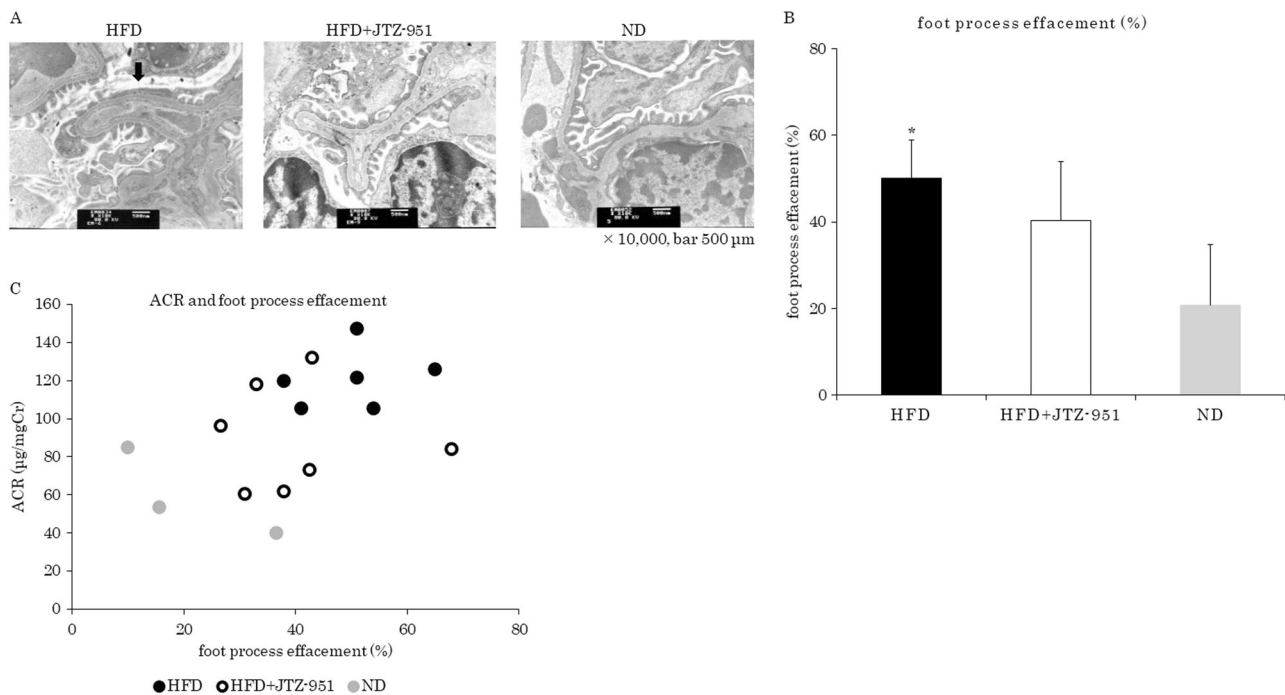


Fig. 7 Podocyte foot process morphology by electron microscopy. **a** Podocyte foot process in the HFD, HFD + JTZ-951, and ND groups. An arrow indicates foot process effacement in the HFD group ($\times 10,000$, bars = 500 μm). **b** The area of foot process effacement (%) was quantitatively evaluated. Data are shown as means \pm SD (HFD, n

= 7; HFD + JTZ-951, $n = 7$; ND, $n = 3$). **c** The relationship between ACR levels and the area of foot process effacement. ACR and foot process effacement were calculated in each mouse and plotted in a single graph. Data are shown as means \pm SD (HFD, $n = 6$; HFD + JTZ-951, $n = 7$; ND, $n = 3$)

epididymal WAT and BW, scores of hepatic steatosis and levels of ACR, although there were no such correlations between plasma adiponectin levels and these parameters. Adiponectin, which is secreted from adipose tissues, has many roles involved in anti-inflammatory, anti-atherosclerotic pathways, in addition to improving insulin sensitivity. Adiponectin is rapidly cleared from the circulation primarily from the liver (in part via the biliary routes) [63], and secondarily from the kidney [64]. In a metabolically challenged status, such as HFD-induced obesity and diabetes with the *ob/ob* background, these mechanisms are perturbed, possibly reflecting a dramatic drop in adiponectin production levels [64]. The net plasma adiponectin levels are downregulated in obesity and appear to contribute to the pathophysiology of insulin resistance, type 2 diabetes, and cardiovascular disease in obese or overweight patients. Plasma adiponectin levels inversely correlated with low-grade albuminuria in humans [65, 66] and mice. In conditions of reduced glomerular filtration rate (GFR), however, adiponectin levels are overall higher and elevated adiponectin is reported as a predictor for mortality in CKD stages 3 and 4 patients [67]. In this study, HFD for 20 weeks resulted in a non-significant increase in plasma creatinine levels (HFD vs. ND group, $P = 0.10$), meaning that GFR was smaller. This might account for the apparent discrepancy of why plasma adiponectin level did not decrease

in the HFD and HFD + JTZ-951 groups, as compared with the ND group. On the other hand, mRNA expression of *adiponectin* in WAT negatively correlated with BW, the degree of hepatic steatosis and ACR levels. These results suggest that an increase in *adiponectin* mRNA by JTZ-951 treatment was associated with improvements in obesity, hepatic steatosis, and glomerular injury. It is also suggested that, in the CKD population, *adiponectin* mRNA expression may have an important predicting value for estimating liver and kidney injury induced by obesity.

The results of the present study should be interpreted within the range of certain limitations. For practical reasons, the sample size for the control animals was small as compared with other groups. Thus, the effects of high-fat diet might have been confounded by type 2 errors. In addition, the statistical tests used generally perform poorly when sample sizes of groups are heterogeneous. Despite these limitations, we firmly believe that the overall anti-obesity effect of PHD inhibitors, as represented by milder adipose inflammation, reductions in hepatic steatosis and glomerular injury, is an important milestone for exploring further the net systemic effects of HIF activation in human clinical settings; multiple lines of human clinical studies of PHD inhibitors are currently ongoing in order to address the therapeutic effect on anemia in CKD.

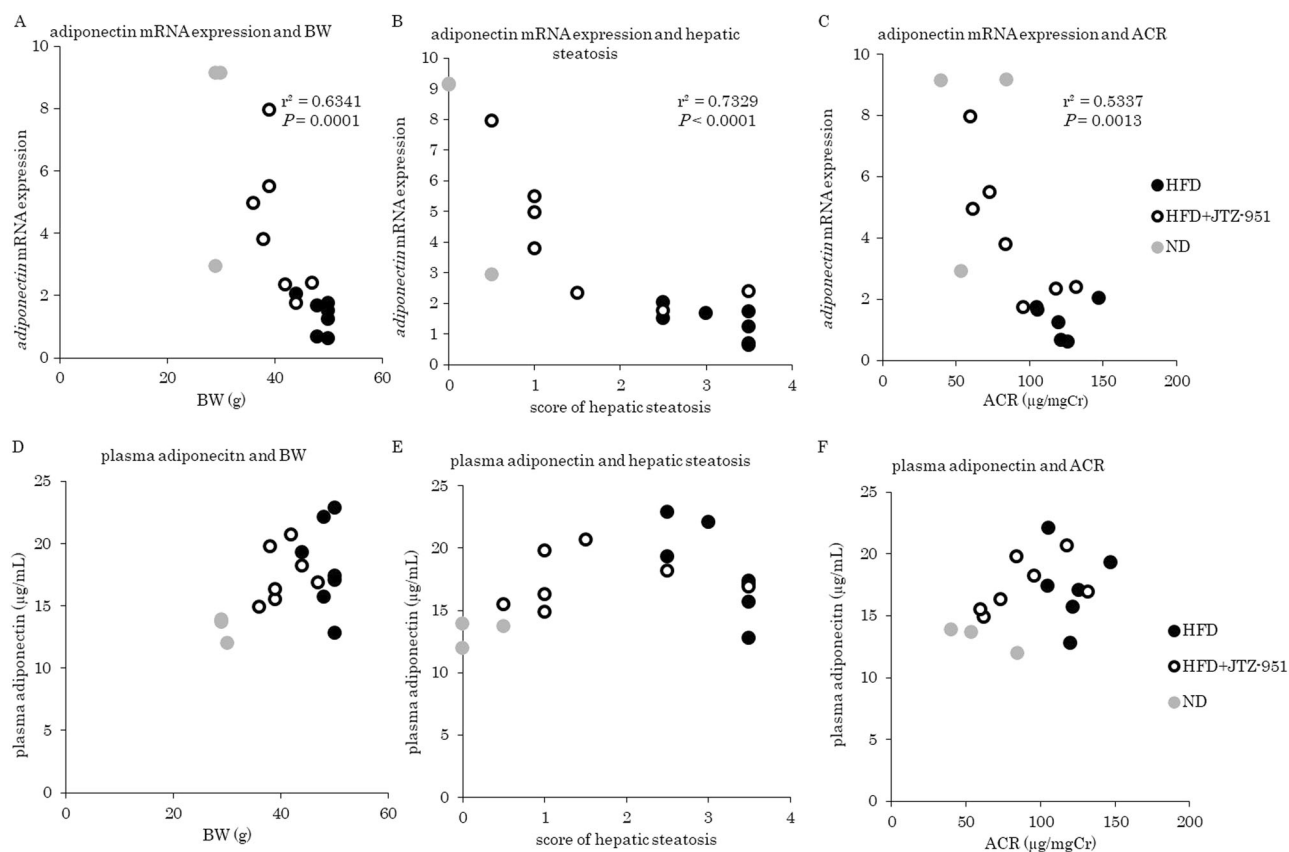


Fig. 8 Inverse correlation between WAT *adiponectin* mRNA and BW, ACR and liver steatosis. **a–f** The relationship between WAT *adiponectin* mRNA and BW (**a**), hepatic steatosis (**b**), and ACR (**c**) was plotted.

In conclusion, PHD inhibition by JTZ-951 treatment improved obesity, plasma levels of nHDL-c, inflammation and interstitial fibrosis in WAT, and hepatic steatosis. In the kidney, JTZ-951 treatment improved pathophysiology of ORG, such as albuminuria, glomerular mesangial expansion, and macrophage infiltration.

These findings support a view that PHD inhibition will be a new therapeutic target for obesity-related diseases. In light of these, it will be an important future step to identify factors and pathways that were influenced by PHD inhibition toward protection.

Acknowledgements We thank Kahoru Amitani and Satoru Fukuda (The University of Tokyo) for technical support. JTZ-951 was provided from Japan Tobacco inc. The study was supported by the Grant-in-Aid for Scientific Research (B, C) from Japan Society for the Promotion of Science 15H04835 (MN) and 17K09688 (TT), the Grant-in-Aid for Scientific Research on Innovative Areas 26111003 (MN) and Biological and Pharmacological Research Laboratories, Central Pharmaceutical Research Institute, Japan Tobacco Inc.

Compliance with ethical standards

Conflict of interest HS, TT, MS, ST, KF, and TW. declare no relationship with any companies that might have a financial interest in the information contained in this paper. MN has honorarium and grants

Similarly, the relationship between plasma adiponectin levels and BW (**d**), hepatic steatosis (**e**), and ACR (**f**) was plotted (HFD, $n = 7$; HFD + JTZ-951, $n = 7$; ND, $n = 3$)

from Astellas, AstraZeneca, Alexion, MSD, Kyowa Hakko Kirin, Daiichi-Sankyo, Mitsubishi-Tanabe, Chugai, Kissei, Kureha, Takeda, Boehringer-Ingelheim, Bayer, Mochida, and JT.

Publisher's note: Springer Nature remains neutral with regard to jurisdictional claims in published maps and institutional affiliations.

References

1. Tanaka S, Tanaka T, Nangaku M. Hypoxia as a key player in the AKI-to-CKD transition. *Am J Physiol Renal Physiol.* 2014;307: F1187–95.
2. Matsumoto M, Makino Y, Tanaka T, Tanaka H, Ishizaka N, Noiri E, et al. Induction of renoprotective gene expression by cobalt ameliorates ischemic injury of the kidney in rats. *J Am Soc Nephrol.* 2003;14:1825–32.
3. Bernhardt WM, Campean V, Kany S, Jurgensen JS, Weidemann A, Warnecke C, et al. Preconditional activation of hypoxia-inducible factors ameliorates ischemic acute renal failure. *J Am Soc Nephrol.* 2006;17:1970–8.
4. Ma D, Lim T, Xu J, Tang H, Wan Y, Zhao H, et al. Xenon preconditioning protects against renal ischemic reperfusion injury via HIF-1 α activation. *J Am Soc Nephrol.* 2009; 20:713–20.
5. Haase VH. Regulation of erythropoiesis by hypoxia-inducible factors. *Blood Rev.* 2013;27:41–53.

6. Cheng K, Ho K, Stokes R, Scott C, Lau SM, Hawthorne WJ, et al. Hypoxia-inducible factor-1 α regulates beta cell function in mouse and human islets. *J Clin Invest.* 2010;120:2171–83.
7. Rankin EB, Rha J, Selak MA, Unger TL, Keith B, Liu Q, et al. Hypoxia-inducible factor 2 regulates hepatic lipid metabolism. *Mol Cell Biol.* 2009;29:4527–38.
8. Zehetner J, Danzer C, Collins S, Eckhardt K, Gerber PA, Ballschmieter P, et al. PVHL is a regulator of glucose metabolism and insulin secretion in pancreatic beta cells. *Genes Dev.* 2008;22:3135–46.
9. Krishnan J, Suter M, Windak R, Krebs T, Felley A, Montessuit C, et al. Activation of a HIF1 α -PPAR γ axis underlies the integration of glycolytic and lipid anabolic pathways in pathologic cardiac hypertrophy. *Cell Metab.* 2009;9:512–24.
10. Provenzano R, Besarab A, Sun CH, Diamond SA, Durham JH, Cangiano JL, et al. Oral Hypoxia-Inducible Factor Prolyl Hydroxylase Inhibitor Roxadustat (FG-4592) for the Treatment of Anemia in Patients with CKD. *Clin J Am Soc Nephrol.* 2016;11:982–91.
11. Provenzano R, Besarab A, Wright S, Dua S, Zeig S, Nguyen P, et al. Roxadustat (FG-4592) Versus Epoetin Alfa for Anemia in Patients Receiving Maintenance Hemodialysis: A Phase 2, Randomized, 6- to 19-Week, Open-Label, Active-Comparator, Dose-Ranging, Safety and Exploratory Efficacy Study. *Am J Kidney Dis.* 2016;67:912–24.
12. Chen N, Qian J, Chen J, Yu X, Mei C, Hao C, et al. Phase 2 studies of oral hypoxia-inducible factor prolyl hydroxylase inhibitor FG-4592 for treatment of anemia in China. *Nephrol Dial Transplant.* 2017;32:1373–86.
13. Akizawa T, Tsubakihara Y, Nangaku M, Endo Y, Nakajima H, Kohno T, et al. Effects of Daprodustat, a Novel Hypoxia-Inducible Factor Prolyl Hydroxylase Inhibitor on Anemia Management in Japanese Hemodialysis Subjects. *Am J Nephrol.* 2017;45:127–35.
14. Marsch E, Demandt JA, Theelen TL, Tullemans BM, Wouters K, Boon MR, et al. Deficiency of the oxygen sensor prolyl hydroxylase 1 attenuates hypercholesterolaemia, atherosclerosis, and hyperglycaemia. *Eur Heart J.* 2016;37:2993–7.
15. Rahtu-Korpela L, Maatta J, Dimova EY, Horkko S, Gylling H, Walkinshaw G, et al. Hypoxia-Inducible Factor Prolyl 4-Hydroxylase-2 Inhibition Protects Against Development of Atherosclerosis. *Arterioscler Thromb Vasc Biol.* 2016;36:608–17.
16. Matsuura H, Ichiki T, Inoue E, Nomura M, Miyazaki R, Hashimoto T, et al. Prolyl hydroxylase domain protein 2 plays a critical role in diet-induced obesity and glucose intolerance. *Circulation.* 2013;127:2078–87.
17. Diet, nutrition and the prevention of chronic disease. [Internet], World Health Organ Tech Rep Ser: Geneva, 2003, [cited 23 April 2003]. Available from http://apps.who.int/iris/bitstream/handle/10665/42665/WHO_TRS_916.pdf;jsessionid=5D986D2FDFD974822EF49A93B20268D7?sequence=1
18. Muoio DM, Newgard CB. Obesity-related derangements in metabolic regulation. *Annu Rev Biochem.* 2006;75:367–401.
19. Poirier P, Giles TD, Bray GA, Hong Y, Stern JS, Pi-Sunyer FX, et al. Obesity and cardiovascular disease: pathophysiology, evaluation, and effect of weight loss. *Arterioscler Thromb Vasc Biol.* 2006;26:968–76.
20. Wolk R, Somers VK. Obesity-related cardiovascular disease: implications of obstructive sleep apnea. *Diabetes Obes Metab.* 2006;8:250–60.
21. Kambham N, Markowitz GS, Valeri AM, Lin J, D'Agati VD. Obesity-related glomerulopathy: an emerging epidemic. *Kidney Int.* 2001;59:1498–509.
22. Chen HM, Liu ZH, Zeng CH, Li SJ, Wang QW, Li LS. Podocyte lesions in patients with obesity-related glomerulopathy. *Am J Kidney Dis.* 2006;48:772–9.
23. Lin S, Thomas TC, Storlien LH, Huang XF. Development of high fat diet-induced obesity and leptin resistance in C57Bl/6J mice. *Int J Obes Relat Metab Disord.* 2000;24:639–46.
24. Buettner R, Scholmerich J, Bollheimer LC. High-fat diets: modeling the metabolic disorders of human obesity in rodents. *Obesity (Silver Spring).* 2007;15:798–808.
25. Ross WR, McGill JB. Epidemiology of obesity and chronic kidney disease. *Adv Chronic Kidney Dis.* 2006;13:325–35.
26. Ogoshi Y, Matsui T, Mitani I, Yokota M, Terashita M, Motoda D, et al. Discovery of JTZ-951: A HIF Prolyl Hydroxylase Inhibitor for the Treatment of Renal Anemia. *ACS Med Chem Lett.* 2017;8:1320–5.
27. Rahtu-Korpela L, Karsikas S, Horkko S, Blanco Sequeiros R, Lammintausta E, Makela KA, et al. HIF prolyl 4-hydroxylase-2 inhibition improves glucose and lipid metabolism and protects against obesity and metabolic dysfunction. *Diabetes.* 2014;63:3324–33.
28. Mallipattu SK, Home SJ, D'Agati V, Narla G, Liu R, Frohman MA, et al. Kruppel-like factor 6 regulates mitochondrial function in the kidney. *J Clin Invest.* 2015;125:1347–61.
29. Jiang T, Wang Z, Proctor G, Moskowitz S, Liebman SE, Rogers T, et al. Diet-induced obesity in C57Bl/6J mice causes increased renal lipid accumulation and glomerulosclerosis via a sterol regulatory element-binding protein-1c-dependent pathway. *J Biol Chem.* 2005;280:32317–25.
30. Hoffer U, Hobbie K, Wilson R, Bai R, Rahman A, Malarkey D, et al. Diet-induced obesity is associated with hyperleptinemia, hyperinsulinemia, hepatic steatosis, and glomerulopathy in C57Bl/6J mice. *Endocrine.* 2009;36:311–25.
31. Hotamisligil GS. Inflammation and metabolic disorders. *Nature.* 2006;444:860–7.
32. Nishimura S, Manabe I, Nagasaki M, Hosoya Y, Yamashita H, Fujita H, et al. Adipogenesis in obesity requires close interplay between differentiating adipocytes, stromal cells, and blood vessels. *Diabetes.* 2007;56:1517–26.
33. Fuentes E, Fuentes F, Vilahur G, Badimon L, Palomo I. Mechanisms of chronic state of inflammation as mediators that link obese adipose tissue and metabolic syndrome. *Mediators Inflamm.* 2013;2013:136584.
34. Meex RCR, Watt MJ. Hepatokines: linking nonalcoholic fatty liver disease and insulin resistance. *Nat Rev Endocrinol.* 2017;13:509–20.
35. Clark JM, Brancati FL, Diehl AM. Nonalcoholic fatty liver disease. *Gastroenterology.* 2002;122:1649–57.
36. Hotta K, Funahashi T, Arita Y, Takahashi M, Matsuda M, Okamoto Y, et al. Plasma concentrations of a novel, adipose-specific protein, adiponectin, in type 2 diabetic patients. *Arterioscler Thromb Vasc Biol.* 2000;20:1595–9.
37. Sharma K, Ramachandrarao S, Qiu G, Usui HK, Zhu Y, Dunn SR, et al. Adiponectin regulates albuminuria and podocyte function in mice. *J Clin Invest.* 2008;118:1645–56.
38. Adamczak M, Chudek J, Wiecek A. Adiponectin in patients with chronic kidney disease. *Semin Dial.* 2009;22:391–5.
39. Strissel KJ, Stancheva Z, Miyoshi H, Perfield JW 2nd, DeFuria J, Jick Z, et al. Adipocyte death, adipose tissue remodeling, and obesity complications. *Diabetes.* 2007;56:2910–8.
40. Murano I, Barbatelli G, Parisani V, Latini C, Muzzonigro G, Castellucci M, et al. Dead adipocytes, detected as crown-like structures, are prevalent in visceral fat depots of genetically obese mice. *J Lipid Res.* 2008;49:1562–8.
41. Cinti S, Mitchell G, Barbatelli G, Murano I, Ceresi E, Faloia E, et al. Adipocyte death defines macrophage localization and function in adipose tissue of obese mice and humans. *J Lipid Res.* 2005;46:2347–55.

42. Tanaka M, Ikeda K, Suganami T, Komiya C, Ochi K, Shirakawa I, et al. Macrophage-inducible C-type lectin underlies obesity-induced adipose tissue fibrosis. *Nat Commun*. 2014;5:4982.
43. Canello R, Clement K. Is obesity an inflammatory illness? Role of low-grade inflammation and macrophage infiltration in human white adipose tissue. *BJOG*. 2006;113:1141–7.
44. Kanda H, Tateya S, Tamori Y, Kotani K, Hiasa K, Kitazawa R, et al. MCP-1 contributes to macrophage infiltration into adipose tissue, insulin resistance, and hepatic steatosis in obesity. *J Clin Invest*. 2006;116:1494–505.
45. Lee KY, Gesta S, Boucher J, Wang XL, Kahn CR. The differential role of Hif1beta/Arnt and the hypoxic response in adipose function, fibrosis, and inflammation. *Cell Metab*. 2011;14:491–503.
46. Lee YS, Kim JW, Osborne O, Oh DY, Sasik R, Schenk S, et al. Increased adipocyte O2 consumption triggers HIF-1alpha, causing inflammation and insulin resistance in obesity. *Cell*. 2014;157:1339–52.
47. Memon RA, Grunfeld C, Feingold KR. TNF-alpha is not the cause of fatty liver disease in obese diabetic mice. *Nat Med*. 2001;7:2–3.
48. Schnyder-Candrian S, Czarniecki J, Lerondel S, Corpataux J, Ryffel B, Schnyder B. Hepatic steatosis in the absence of tumor necrosis factor in mice. *Cytokine*. 2005;32:287–95.
49. Teoh N, Field J, Farrell G. Interleukin-6 is a key mediator of the hepatoprotective and pro-proliferative effects of ischaemic preconditioning in mice. *J Hepatol*. 2006;45:20–7.
50. Yamaguchi K, Itoh Y, Yokomizo C, Nishimura T, Niimi T, Umemura A, et al. Blockade of IL-6 signaling exacerbates liver injury and suppresses antiapoptotic gene expression in methionine choline-deficient diet-fed db/db mice. *Lab Invest*. 2011;91:609–18.
51. Wei K, Pieciewicz SM, McGinnis LM, Taniguchi CM, Wiegand SJ, Anderson K, et al. A liver Hif-2alpha-Irs2 pathway sensitizes hepatic insulin signaling and is modulated by Vegf inhibition. *Nat Med*. 2013;19:1331–7.
52. Taniguchi CM, Finger EC, Krieg AJ, Wu C, Diep AN, LaGory EL, et al. Cross-talk between hypoxia and insulin signaling through Phd3 regulates hepatic glucose and lipid metabolism and ameliorates diabetes. *Nat Med*. 2013;19:1325–30.
53. Heiker JT, Kosel D, Beck-Sickinger AG. Molecular mechanisms of signal transduction via adiponectin and adiponectin receptors. *Biol Chem*. 2010;391:1005–18.
54. Targher G, Bertolini L, Scala L, Poli F, Zenari L, Falezza G. Decreased plasma adiponectin concentrations are closely associated with nonalcoholic hepatic steatosis in obese individuals. *Clin Endocrinol (Oxf)*. 2004;61:700–3.
55. Polyzos SA, Kountouras J, Zavos C, Tsiaousi E. The role of adiponectin in the pathogenesis and treatment of non-alcoholic fatty liver disease. *Diabetes Obes Metab*. 2010;12:365–83.
56. Polyzos SA, Mantzoros CS. Adiponectin as a target for the treatment of nonalcoholic steatohepatitis with thiazolidinediones: A systematic review. *Metabolism*. 2016;65:1297–306.
57. Sadiku P, Willson JA, Dickinson RS, Murphy F, Harris AJ, Lewis A, et al. Prolyl hydroxylase 2 inactivation enhances glycogen storage and promotes excessive neutrophilic responses. *J Clin Invest*. 2017;127:3407–20.
58. Semba H, Takeda N, Isagawa T, Sugiura Y, Honda K, Wake M, et al. HIF-1alpha-PDK1 axis-induced active glycolysis plays an essential role in macrophage migratory capacity. *Nat Commun*. 2016;7:11635.
59. Kobayashi H, Gilbert V, Liu Q, Kapitsinou PP, Unger TL, Rha J, et al. Myeloid cell-derived hypoxia-inducible factor attenuates inflammation in unilateral ureteral obstruction-induced kidney injury. *J Immunol*. 2012;188:5106–15.
60. D'Agati VD. Podocyte injury in focal segmental glomerulosclerosis: Lessons from animal models (a play in five acts). *Kidney Int*. 2008;73:399–406.
61. Kwok C, Shannon MB, Miner JH, Shaw A. Pathogenesis of nonimmune glomerulopathies. *Annu Rev Pathol*. 2006;1:349–74.
62. Susztak K, Raff AC, Schiffer M, Bottinger EP. Glucose-induced reactive oxygen species cause apoptosis of podocytes and podocyte depletion at the onset of diabetic nephropathy. *Diabetes*. 2006;55:225–33.
63. Darouich S, Goucha R, Jaafoura MH, Zekri S, Ben Maiz H, Kheder A. Clinicopathological characteristics of obesity-associated focal segmental glomerulosclerosis. *Ultrastruct Pathol*. 2011;35:176–82.
64. Ritz E, Koleganova N, Piecha G. Is there an obesity-metabolic syndrome related glomerulopathy? *Curr Opin Nephrol Hypertens*. 2011;20:44–9.
65. Tacke F, Wustefeld T, Horn R, Luedde T, Srinivas Rao A, Manns MP, et al. High adiponectin in chronic liver disease and cholestasis suggests biliary route of adiponectin excretion in vivo. *J Hepatol*. 2005;42:666–73.
66. Halberg N, Schraw TD, Wang ZV, Kim JY, Yi J, Hamilton MP, et al. Systemic fate of the adipocyte-derived factor adiponectin. *Diabetes*. 2009;58:1961–70.
67. Tsioufis C, Dimitriadis K, Chatzis D, Vasiliadou C, Tousoulis D, Papademetriou V, et al. Relation of microalbuminuria to adiponectin and augmented C-reactive protein levels in men with essential hypertension. *Am J Cardiol*. 2005;96:946–51.